Time Dependent Density Functional Theory Study of Electronic Absorption Properties of Lead(II) Complexes with a Series of Hydroxyflavones

C. Lapouge and J. P. Cornard*

LASIR, CNRS UMR 8516, Université des Sciences et Technologies de Lille, Bât C5, 59655 Villeneuve d'Ascq Cedex, France

Received: May 13, 2005; In Final Form: June 8, 2005

The structural changes occurring with the chelation of lead(II) to 3-hydroxyflavone, 5-hydroxyflavone, and 3′,4′-dihydroxyflavone have been investigated by the density functional theory (DFT) method with the B3LYP functional and the 6-31G(d,p) basis set. The two effective core potentials Lanl2dz (Los Alamos) and MWB78 (Stuttgart/Dresden) were used for the Pb ion. Only the 3′,4′-dihydroxyflavone ligand shows minor geometrical modifications upon chelation, whereas the two other ligands present important changes of their chromone moiety. The time dependent density functional theory (TD-DFT) has been employed to calculate the electronic absorption spectra of the 1:1 complexes of lead(II) with the three hydroxyflavones, as well in a vacuum as in methanol. The solvent effect is modeled using the self-consistent reaction field (SCRF) method with the polarized continuum model (PCM). Comparison with experimental data allows a precise assessment of the performances of the method, which appears competitive and suitable to reproduce the spectral measurements when the solvent effect is taken into account. These calculations and the molecular orbital analysis have allowed an explanation of the different behaviors of the three ligands toward Pb(II) and particularly the fact that no bathochromic shift is observed with the addition of lead(II) to a 5-hydroxyflavone solution. A complete assignment of the electronic absorption spectra of both free and complexed ligands has been carried out.

1. Introduction

Humic substances (HS) are a naturally occurring mixture of organic compounds, ubiquitous in nature, which play an important role in both pollutant chemistry and the biochemistry of natural waters and soils.[1,2] HS are known to significantly affect the behavior of some pollutants in natural environments such as trace metal speciation and toxicity.[3−5] HS contain a large number of different complexing sites in competition. The carboxylic, phenolic, and carbonyl functions are the most abundant and most influential in regard to metal complexation.[6] However, size, heterogeneity and multiplicity of possible interaction sites of HS often make it difficult to predict a specific behavior for metal−HS interactions. For these reasons, investigations of much simpler systems which are commonly known as precursors of HS are reported in the literature.[7−11] Previous studies have shown that polyphenols and notably flavonoids are not negligible components of HS.[12−15] Flavonoids, 2-phenyl-benzo-α-pyrones, are polyphenolic compounds that occur ubiquitously in the plant kingdom and, more precisely, are secondary metabolites of higher plants.[16,17] A multitude of substitution patterns in the two benzene rings (A and B) of the basic structure occur in nature. Over 4000 different naturally occurring flavonoids have been described, and this list is still growing. The individual compounds within each class are distinguished mainly by the number and orientation of hydroxyl, methoxyl, and other groups substituted in the two benzene rings. The flavonoid molecules which present hydroxyl functions enable the formation of complexes with metals. This property has been extensively used in analytical methods for the determination and dosage of metal traces in solution.[18−20] The main chelating sites occurring in flavonoids are respectively the 3-hydroxy-4-keto, 5-hydroxy-4-keto, and ortho-dihydroxyl (catechol) groups.

In previous works, we focused our attention on the aluminium(III) complexation study with mono- and poly-hydroxylated flavones. The complexation mechanisms of molecules presenting only one binding site—3-hydroxyflavone (3HF), 5-hydroxyflavone (5HF), and 3′,4′-dihydroxyflavone (3′,4′-diHF)—have been investigated. Then, the study of Al(III) complexation with quercetin and isoquercitrin that simultaneously possess three and two chelating sites in competition has been realized. These works reporting the structural and spectroscopic investigation of each complex have allowed (i) classification of the groups according to their ability to form a chelate when the sites are individually taken and (ii) verification that the classification is still valid when these sites are in competition within only one ligand.[21−26] In these studies, quantum chemical calculations (density functional theory (DFT) and time dependent density functional theory (TD-DFT)) have been performed in order to serve as support for the interpretation of experimental data obtained by molecular spectroscopic methods (vibrational and electronic). In the second step of our work, we were interested in the chelation of lead(II) by model molecules such as caffeic acid[27] but also hydroxyflavones. Recently, we published a paper concerning the comparison of the chelating power of the α-hydroxy-carbonyl, *β*-hydroxy-carbonyl, and catechol sites in relation to Pb(II) in methanol solution.[28] The stoichiometric composition and the stability constant of each complex obtained with 3HF, 5HF, and 3′,4′-diHF have been established by UV−visible spectroscopy combined with chemometric methods. The results of this study show that for lead(II) complexation the behaviors of the three ligands radically differ. Notably, the spectral modifications engendered by the chelation are not easily interpretable, although they made it possible to clearly visualize

* Corresponding author. Phone: +33-3.20.43.69.26. Fax: +33-3.20.43.67.55. E-mail: cornard@univ-lille1.fr.

10.1021/jp0525235 CCC: $30.25
Published on Web 07/08/2005

TABLE 1: Calculated Bond and H-Bond Lengths (Å) of the 3HF, 5HF, and 3′,4′-diHF Ligands and Their 1:1 Complex with Pb^{2+} Obtained with the Lanl2dz ECP[a]

	3HF	[Pb(3HF)]$^+$	5HF	[Pb(5HF)]$^+$	3′,4′-diHF	Pb(3′,4′-diHF)
O_1C_2	1.377	1.348	1.361	1.346	1.366	1.367
C_2C_3	1.369	1.406	1.361	1.379	1.361	1.361
C_3C_4	1.462	1.422	1.447	1.412	1.455	1.455
C_4C_{10}	1.455	1.429	1.458	1.440	1.481	1.482
$C_{10}C_5$	1.408	1.413	1.422	1.435	1.403	1.404
C_5C_6	1.383	1.382	1.399	1.397	1.387	1.387
C_6C_7	1.408	1.411	1.395	1.395	1.405	1.405
C_7C_8	1.386	1.386	1.396	1.393	1.389	1.389
C_8C_9	1.401	1.398	1.391	1.389	1.398	1.399
C_9C_{10}	1.403	1.408	1.404	1.419	1.400	1.400
C_9O_1	1.359	1.362	1.374	1.368	1.372	1.370
$C_2C_{1'}$	1.468	1.456	1.476	1.461	1.472	1.473
$C_{1'}C_{2'}$	1.410	1.414	1.406	1.410	1.410	1.405
$C_{2'}C_{3'}$	1.393	1.390	1.391	1.390	1.384	1.393
$C_{3'}C_{4'}$	1.395	1.397	1.397	1.398	1.409	1.423
$C_{4'}C_{5'}$	1.396	1.399	1.395	1.397	1.392	1.401
$C_{5'}C_{6'}$	1.391	1.388	1.393	1.390	1.393	1.389
$C_{6'}C_{1'}$	1.409	1.415	1.406	1.410	1.404	1.413
C_4O_4	1.243	1.308	1.251	1.306	1.232	
C_3O_3	1.352	1.341				
O_3H_3	0.985					
C_5O_5			1.338	1.340		
O_5H_5			0.998			
$C_{3'}O_{3'}$					1.375	1.348
$O_{3'}H_{3'}$					0.965	
$C_{4'}O_{4'}$					1.356	1.343
$O_{4'}H_{4'}$					0.970	
O_3Pb		2.082 (2.151)				
O_4Pb		2.136 (2.204)		2.116 (2.186)		
O_5Pb				2.037 (2.106)		
$O_{3'}Pb$						2.070 (2.141)
$O_{4'}Pb$						2.080 (2.151)
$O_4\cdots H_5$			1.684			
$O_4\cdots H_3$	1.936					
$O_3\cdots H_{2'}$	2.159	2.166				
$O_{3'}\cdots H_{4'}$					2.120	

[a] The values in parentheses are relative to calculations performed with the MWB78 ECP.

the formation of various complexes. For these reasons, the purpose of this paper is (i) to determine the structural changes of the ligands occurring with Pb(II) complexation and (ii) to explain the spectral shifts observed in the electronic spectra of 3HF, 5HF, and 3′,4′-diHF with the addition of lead chloride. Only the predominant complexed form of stoichiometry 1:1 for each ligand has been studied by quantum chemical calculations at the DFT and TD-DFT levels of theory. The theoretical electronic spectra of complexes are compared to the experimental ones obtained by chemometric analysis (evolving factor analysis)[29] and presented in our previous paper.[28] Another fundamental goal of this work is to demonstrate the possibility and accuracy of TD-DFT calculations to reproduce experimental electronic spectra of lead(II) complexes by taking into account the solvent effects. Indeed, until today, no study of this type has been reported in the literature and this work constitutes a good first test of validity.

2. Calculations

The DFT calculations have been performed with the Gaussian 03 quantum chemical package[30] implemented on a IBM SP/Power 4 machine located at IDRIS (CNRS, France). Geometry optimizations of hydroxyflavones and their 1:1 complexes with Pb(II) were obtained by using the three-parameter hybrid functional B3LYP.[31,32] For Pb, we adopted the Los Alamos double-ξ (Lanl2dz) and quasi-relativistic Stuttgart/Dresden (MWB78) effective core potentials (ECPs) and the 6-31G(d,p) basis set for the other atoms (including polarization functions, to correctly take into account intramolecular H-bonding). For all compounds, vibrational frequency calculations have been performed to ensure that the optimized structures correspond to energy minima. The low-lying excited states were treated within the adiabatic approximation of time dependent density functional theory (DFT-RPA)[33] with the B3LYP hybrid functional. Vertical excitation energies were computed for the first 40 singlet excited states, to reproduce the UV−visible spectra of free and complexed molecules. Solvent effects on calculated UV−visible spectra were introduced by the self-consistent reaction field (SCRF) method, via the polarized continuum model (PCM)[34] implemented in the Gaussian program. In result, only transitions presenting high oscillator strengths (≥ 0.1) have been considered without focusing on their relative values, because it is well-known that, in such calculations, relative oscillator strengths are not reliable. The molecular orbitals (MOs) involved in the main calculated electronic transitions have been drawn using the GaussView 3.09 program. One can note that the MOs calculated in a vacuum and in methanol differ in energy but not in shape.

3. Results and Discussion

3.1. Structural Analysis. The calculated geometrical parameters of the three studied hydroxyflavones and their 1:1 complex with lead(II) are reported in Tables 1 (bond lengths) and 2 (bond and dihedral angles). Only the inter-ring dihedral angles are specified, since the other parts of the molecules (chromone and B ring) are planar for all of the optimized geometries. The lengths of the intramolecular hydrogen bonds are also reported in Table 1. The atomic numbering used in the text is reported in Figure 1; all of the H atoms and the OH groups have the same number as the C atom to which they are linked.

TABLE 2: Calculated Bond and Twist Angles (deg) of the 3HF, 5HF, and 3′,4′-diHF Ligands and Their 1:1 Complex with Pb^{2+} (Lanl2dz ECP)

	3HF	$[Pb(3HF)]^+$	5HF	$[Pb(5HF)]^+$	3′,4′-diHF	Pb(3′,4′-diHF)
$O_1C_2C_3$	119.0	117.9	121.4	119.6	121.3	121.2
$C_2C_3C_4$	122.4	120.1	121.7	121.4	122.8	122.8
$C_3C_4C_{10}$	116.0	120.2	115.8	118.8	113.9	113.9
$C_4C_{10}C_9$	118.4	116.7	119.9	117.0	119.7	119.7
$C_9C_{10}C_5$	119.1	118.9	118.8	117.5	118.7	118.7
$C_{10}C_5O_6$	120.2	119.6	119.4	119.3	120.5	120.5
$C_5C_6C_7$	119.9	120.4	119.8	120.8	119.8	119.8
$C_6C_7C_8$	121.0	121.1	122.1	121.4	120.7	120.7
$C_7C_8C_9$	118.8	118.2	117.8	118.1	118.8	118.8
$C_8C_9C_{10}$	121.0	121.8	122.2	122.9	121.5	121.5
$C_{10}C_9O_1$	122.0	120.8	120.6	121.0	121.9	121.9
$C_9O_1C_2$	122.2	124.3	121.0	122.1	120.4	120.4
$C_1C_2C_{1'}$	112.4	113.4	112.2	113.8	112.0	112.1
$C_2C_{1'}C_{2'}$	121.7	121.9	121.1	120.7	120.8	120.7
$C_{1'}C_{2'}C_{3'}$	120.3	120.2	120.8	120.8	120.5	120.2
$C_{2'}C_{3'}C_{4'}$	120.7	120.5	120.3	120.1	120.7	120.2
$C_{3'}C_{4'}C_{5'}$	119.4	119.9	119.6	120.1	119.1	119.4
$C_{4'}C_{5'}C_{6'}$	120.4	120.2	120.3	120.2	120.3	119.9
$C_{5'}C_{6'}C_{1'}$	120.7	120.5	120.5	120.2	121.0	121.2
$C_{6'}C_{1'}C_{2'}$	118.4	118.8	118.6	119.1	118.4	119.0
$C_3C_4O_4$	118.3	118.0	122.7	117.4	123.4	123.6
$C_4C_3O_3$	113.5	116.6				
$C_3O_3H_3$	102.7					
$C_{10}C_5O_5$			120.5	122.8		
$C_5O_5H_5$			106.3			
$C_{4'}C_{3'}O_{3'}$					114.5	117.4
$C_{3'}O_{3'}H_{3'}$					110.2	
$C_{3'}C_{4'}O_{4'}$					120.4	117.6
$C_{4'}O_{4'}H_{4'}$					107.7	
C_3O_3Pb		114.7				
C_4O_4Pb		113.4		128.6		
C_5O_5Pb				131.7		
$C_{3'}O_{3'}Pb$						112.6
$C_{4'}O_{4'}Pb$						112.4
$C_3C_2C_{1'}C_{2'}$	0.0	0.0	19.9	6.7	17.0	18.5

Comparison of the bond lengths of the free ligands shows that substitution of a hydroxyl group on the A or C ring affects these two moieties but not the B ring, and vice versa, substitutions on the B ring do not perturb the two others. The inter-ring bond $C_2C_{1'}$ varies only a little between the three species, showing a relative electronic independence of the chromone part on one hand and the B ring on the other hand. The C═O bond length is different in each compound, due to the presence and the force of H-bonds with this oxygen atom. Its length is maximal in 5HF (strong H-bond), decreases in 3HF (weaker H-bond), and is minimal in 3′,4′-diHF (no H-bond). For this latter ligand, the $O_{3'}\cdots H_{4'}$ hydrogen bonding induces a longer bond length for $C_{3'}O_{3'}$ than for $C_{4'}O_{4'}$.

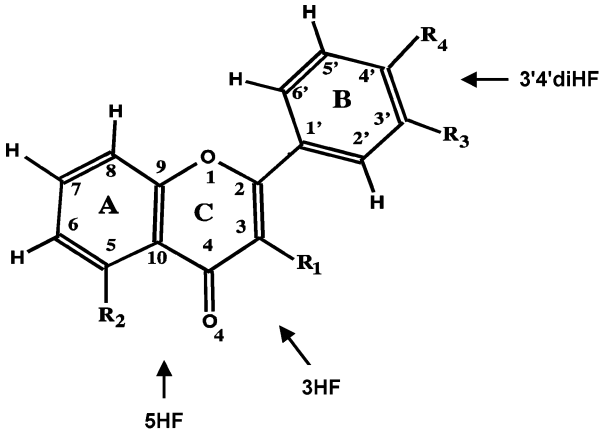

Figure 1. Atomic numbering of hydroxyflavones (IUPAC nomenclature). 3-Hydroxyflavone: $R_1 = OH$, $R_2 = R_3 = R_4 = H$. 5-Hydroxyflavone: $R_2 = OH$, $R_1 = R_3 = R_4 = H$. 3′,4′-Dihydroxyflavone: $R_3 = R_4 = OH$, $R_1 = R_2 = H$. The arrows indicate the possible chelating sites of Pb(II).

Calculated angles show only a few significant variations between the ligands, and they essentially concern the C ring. Due to the presence of the low intramolecular H-bond

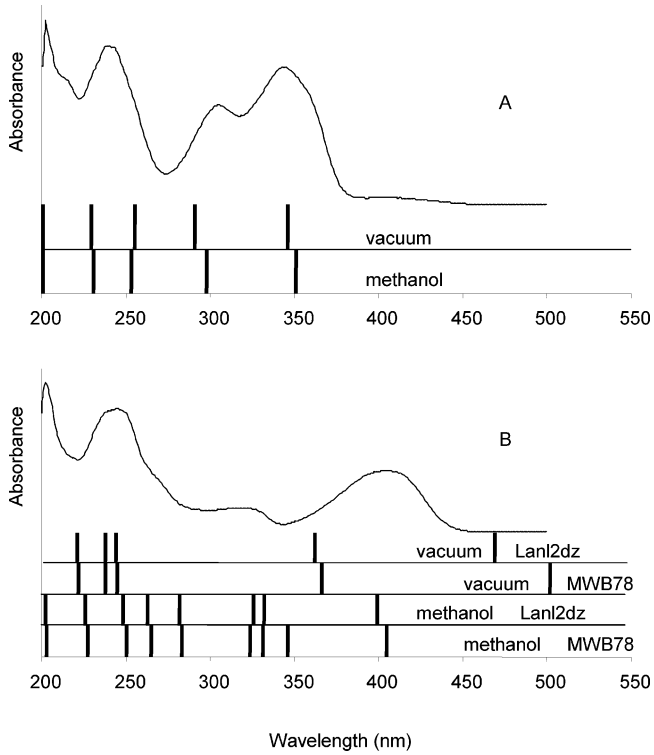

Figure 2. UV−visible spectrum recorded in methanol[23] and positions of the electronic transitions calculated in a vacuum and in methanol of (A) 3HF and (B) $[Pb(3HF)]^+$ (both Lanl2dz and MWB78 pseudopotentials for Pb are used in calculations on this complex).

TABLE 3: Experimental and Calculated[a] (in a Vacuum and in Methanol) Wavelengths (nm) for 3HF and [Pb(3HF)]$^+$ [b]

3HF									[Pb(3HF)]$^+$								
	calcd									calcd							
exptl	vacuum					methanol				exptl	vacuum				methanol				
λ	λ	MO	%	f		λ	MO	%	f	λ	λ	MO	%	f		λ	MO	%	f
344	346	H → L	79	0.36		351	H → L	82	0.46	405	469	H → L	84	0.19		399	H → L	81	0.52
302	291	H − 1 → L	83	0.11		298	H − 1 → L	88	0.15	322	362	H → L + 1	72	0.45		332	H − 1 → L	46	0.15
242	255	H → L + 2	83	0.10		253	H − 3 → L	47	0.14								H → L + 1	24	
		H − 4 → L	10				H → L + 2	19									H − 2 → L	21	
							H → L + 1	15								326	H − 2 → L	72	0.16
237	229	H − 1 → L + 1	68	0.16		231	H − 1 → L + 1	70	0.17								H − 1 → L	13	
		H − 5 → L	12				H − 5 → L	11		266						282	H − 3 → L	76	0.10
215[c]	211[d]					211[d]											H → L + 2	18	
201	201	H − 1 → L + 3	31	0.14		201	H − 2 → L + 2	40	0.29							263	H − 4 → L	56	0.11
		H − 2 → L + 2	22				H − 1 → L + 2	23									H → L + 2	16	
		H − 5 → L + 1	13				H − 5 → L + 1	10									H − 1 → L + 1	13	
		H − 1 → L + 2	12							243	244	H → L + 3	47	0.19		248	H → L + 2	45	0.17
												H − 2 → L + 3	15				H − 4 → L	21	
												H− 3 → L + 1	13						
										236	238	H → L + 5	48	0.15		226	H − 1 → L + 2	56	0.16
												H − 2 → L + 3	30				H → L + 4	10	
										202	221	H → L + 5	43	0.15		202	H − 8 → L	61	0.12
												H − 2 → L + 3	33				H − 4 → L + 2	13	

[a] Only transitions with an oscillator strength ≥0.1 and molecular orbitals with a contribution ≥10% are reported. [b] f: calculated oscillator strength. [c] Shoulder. [d] Oscillator strength <0.1.

TABLE 4: Energies (eV) of the Molecular Orbitals of [Pb(3HF)]$^+$ Calculated in a Vacuum and in Methanol with Both the Lanl2dz and MWB78 Pseudopotentials

		H − 8	H − 4	H − 3	H − 2	H − 1	H	L	L + 1	L + 2	L + 3	L + 4	L + 5
vacuum	Lanl2dz			−0.399	−0.369		−0.345	−0.235	−0.208		−0.151		−0.125
	MWB78			−0.397	−0.367		−0.343	−0.239	−0.207		−0.149		−0.124
methanol	Lanl2dz	−0.363	−0.297	−0.288	−0.264	−0.259	−0.230	−0.104	−0.073	−0.039		−0.017	
	MWB78	−0.360	−0.295	−0.286	−0.263	−0.258	−0.227	−0.102	−0.074	−0.038		−0.016	

$O_3 \cdots H_{2'}$ (2.159 Å) between the B ring and the chromone part, only 3HF is planar. The B ring of 5HF and of 3′,4′-diHF is twisted relative to the chromone part by 19.9 and 17.0°, respectively. Meyer[35] has reported twist angles of 22 and 27° for 3HF and 5HF, respectively, but this author has used the HF/6-31G(d) level of theory and this basis set does not include the polarization orbitals on H atoms, necessary to properly describe the hydrogen bonding. Petroski et al.[36] have calculated the structure of a 3HF−water system at the B3LYP/6-31G(d) level and have found a dihedral angle of 11.9° between the phenyl ring and the remainder of the molecule, but this calculation presents the same weakness as the previous one. Finally, Premvardhan et al. reported a planar structure for 3HF obtained by calculations at the HF/6-31+G(2d,p) level.[37]

Previous studies concerning the complexation of a metal ion by hydroxyflavones report the formation of a chelate with a complete deprotonation of the hydroxyl functions at the chelating site level.[21−25,38−42] Thus, we can assume that the complexation of Pb(II) by each studied ligand also leads to chelate formation with deprotonation of the hydroxyl groups. Only the structural parameters of the chelates obtained with the Lanl2dz effective core potential are reported in Tables 1 and 2. In the complexes, the geometrical parameters (bond lengths, bond and dihedral angles) of the ligands do not appreciably differ according to the pseudopotential used; only variations of 0.002 Å are observed for the bond lengths. In opposition, the Pb−O bond length is sensitive to the effective core potential used in the geometry optimization, and the calculated bond lengths obtained with MWB78 are also reported in Table 1. The average Pb−O bond lengths are calculated 0.07 Å longer with MWB78 than with Lanl2dz. This dependency of bond lengths on pseudopotential has already been observed by Salpin et al.[43]

Complexation of 3HF induces drastic changes in the γ-pyrone ring with important variations of all the angles and bond lengths, except the C_9C_{10} and C_9O_1 ones that increase by only 0.005 and 0.003 Å, respectively. The shortening of 0.029 Å of the O_1C_2 bond length is accompanied by an electronic delocalization on C atoms 2, 3, 4, and 10, more pronounced than in free 3HF, and a non-negligible decrease of the inter-ring bond (0.012 Å). The C_4O_4 bond loses its double bond character with a length equal to 1.308 Å. Upon complexation, the A and B rings are not affected; the ligand remains planar with a small decrease of the strength of the intramolecular H-bond. Chelation of Pb(II) to 3HF gives rise to a planar, five-membered ring in which the two CO and PbO bonds are not identical and differ by 0.033 and 0.054 Å, respectively.

In $[Pb(5HF)]^+$, the same preponderant modifications can be observed: the C ring is the most affected, to a lesser extent but with the same trends as those in the $[Pb(3HF)]^+$ complex. The A ring is affected only via the increase of the $C_{10}C_5$ and C_9C_{10} bond lengths and a decrease of 1.3° of the $C_9C_{10}C_5$ angle. As previously mentioned, the inter-ring bond is significantly shortened. In this complex, lead is involved in a planar, six-membered ring in which CO bonds have similar lengths as those in $[Pb(3HF)]^+$, but the PbO bonds are shorter. In the complex, the inter-ring dihedral angle is considerably reduced (6.7°) with respect to the free ligand. However, pyronium and cinnamoyl resonant forms are not observed for the complexed ligand, contrary to the case of the $[Al(5HF)]^{2+}$ chelate.[23]

In opposition to the two other hydroxyflavones, coordination of Pb(II) to the catechol group shows only minor effects on the geometrical parameters of 3′,4′-diHF. The greatest modification concerns the $C_{3'}C_{4'}$ bond that lengthens by 0.014 Å. The B ring remains twisted with respect to the chromone moiety, with a small increase of the dihedral angle. The two CO bonds of the five-membered ring containing Pb(II) reach approximately the same values, as well as the two PbO ones.

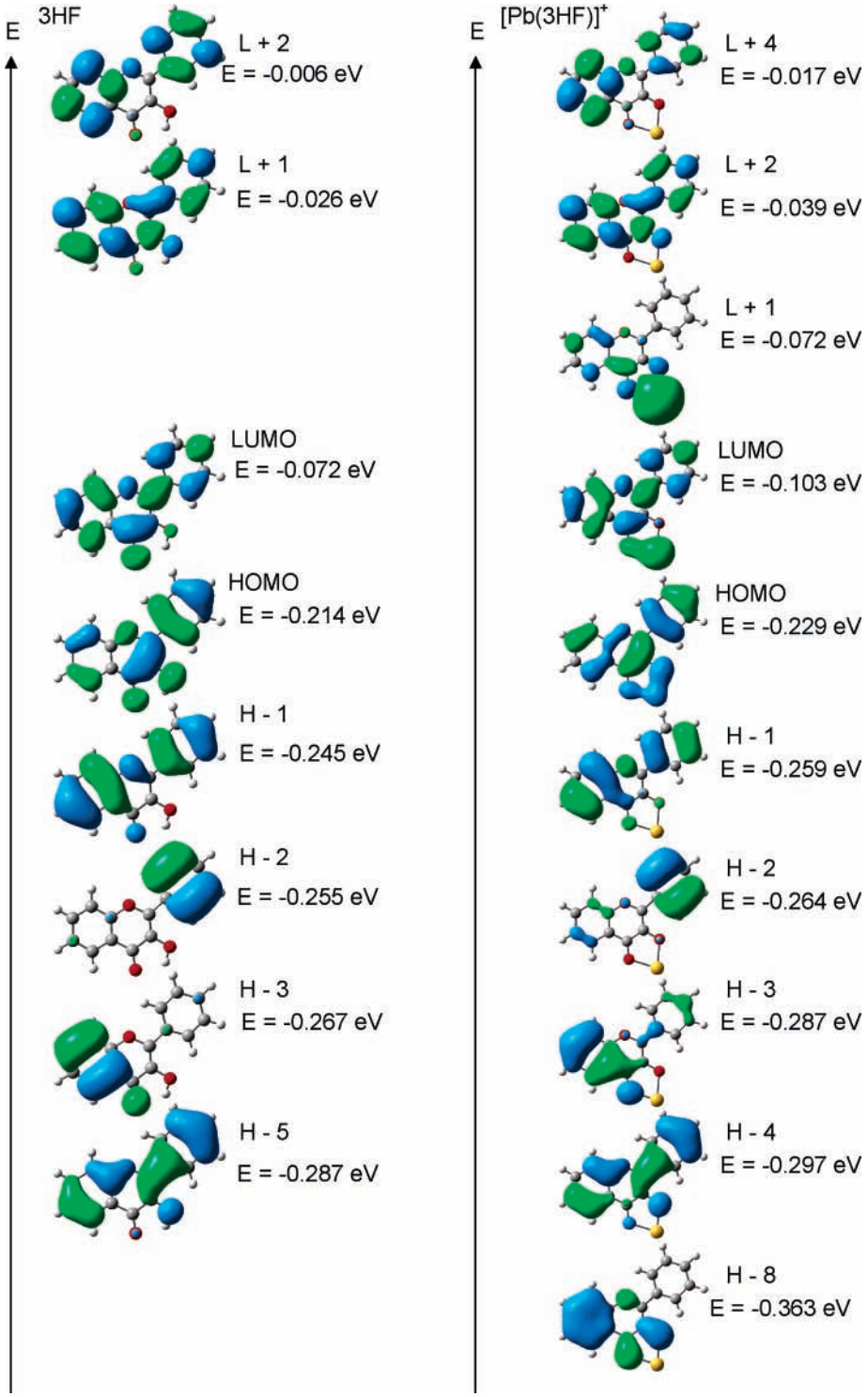

Figure 3. Molecular orbitals of 3HF and $[Pb(3HF)]^+$ calculated in methanol.

3.2. Electronic Spectra and Molecular Orbital Analysis. *3-Hydroxyflavone.* The experimental electronic spectrum of the free ligand is reported in Figure 2, part A, with the theoretical ones calculated both in a vacuum and with the solvent effect (methanol). The two calculated spectra are very similar and in good accordance with the experimental feature. Five transitions are calculated, and each of them can be associated with an observed band. The 215 nm shoulder present in the absorption spectrum is calculated at 211 nm in a vacuum and in methanol (Table 3), but it is not represented in Figure 2 because of its low oscillator strength. The three lowest wavelengths have almost the same calculated values in a vacuum and in methanol (within 2 nm) and correspond to $\lambda = 201$, 237, and 242 nm experimentally. On the other hand, the two others are relatively different. $\lambda_{exptl} = 302$ nm is better reproduced in methanol at 298 nm (291 in a vacuum), whereas the calculation in a vacuum gives a transition located at 346 nm, closer to $\lambda_{exptl} = 344$ nm than the result calculated in methanol (351 nm). Table 3 presents the wavelengths observed in methanol and calculated both in a vacuum and in methanol for the electronic transitions having an oscillator strength higher than 0.1. For each theoretical wavelength, the molecular orbitals involved in the transition with a contribution $\geq 10\%$ are also mentioned. One can see that three transitions have preponderant contributions of the same

TABLE 5: Experimental and Calculated[a] (in a Vacuum and in Methanol) Wavelengths (nm) for 5HF and [Pb(5HF)]$^+$ [b]

5HF									[Pb(5HF)]$^+$								
	calcd									calcd							
exptl	vacuum					methanol				exptl	vacuum					methanol			
λ	λ	MO	%	f		λ	MO	%	f	λ	λ	MO	%	f		λ	MO	%	f
337	366	H → L	93	0.10		356	H → L	92	0.11	335	379	H → L + 1	83	0.15		344	H → L + 1	93	0.13
298	284	H − 2 → L	45	0.20		294	H − 1 → L	81	0.60		333	H − 1 → L + 1	62	0.36		326	H − 1 → L	86	0.63
		H − 1 → L	25									H − 2 → L + 1	23						
		H → L + 1	19								330	H − 2 → L + 1	70	0.14					
270	278	H − 1 → L	49	0.46		275	H → L + 1	60	0.16			H − 1 → L + 1	18						
		H → L + 1	30				H − 3 → L	25		296						280	H → L + 2	43	0.16
						262	H − 3 → L	36	0.17								H − 1 → L + 1	33	
							H − 2 → L	24									H − 3 → L	16	
							H → L + 1	20		268	269	H − 4 → L	88	0.11		268	H − 3 → L	65	0.20
212	210	H → L + 3	21	0.10		210	H → L + 3	35	0.10	241	256	H − 1 → L + 3	63	0.23		244	H − 1 → L + 2	55	0.22
		H − 2 → L + 1	21				H − 3 → L + 3	24				H − 3 → L + 1	23				H − 3 → L + 1	36	
		H → L + 4	17							202	203	H − 1 → L + 5	25	0.10		206	H − 1 → L + 4	34	0.21
		H − 2 → L + 2	14									H − 3 → L + 3	22				H − 3 → L + 2	12	
201	202	H − 2 → L + 2	26	0.11		206	H − 1 → L + 2	47	0.17			H − 1 → L + 6	11						
		H − 4 → L + 1	26				H − 2 → L + 1	13											
		H − 1 → L + 2	14																

[a] Only transitions with an oscillator strength ≥0.1 and molecular orbitals with a contribution ≥10% are reported. [b] f: calculated oscillator strength.

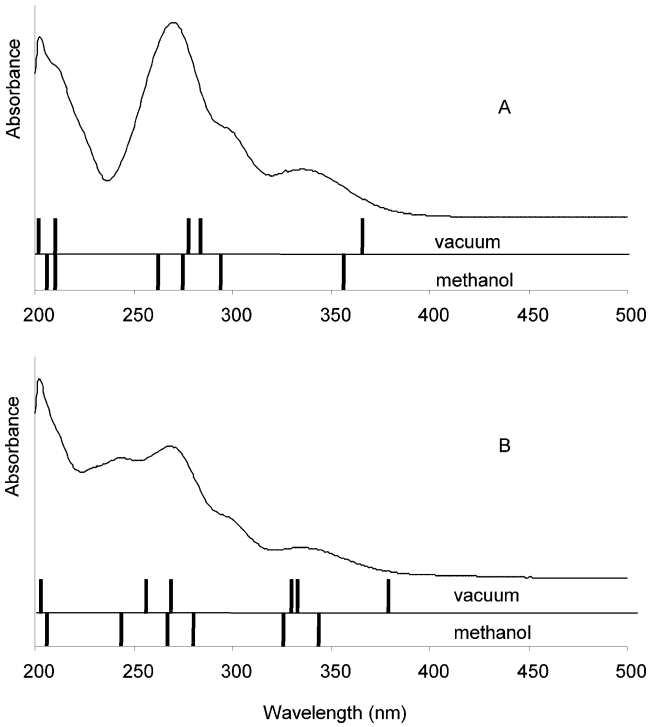

Figure 4. UV−visible spectrum recorded in methanol[23] and positions of the electronic transitions calculated in a vacuum and in methanol of (A) 5HF and (B) [Pb(5HF)]$^+$.

molecular orbitals both in a vacuum and in methanol (346 and 351 nm; 291 and 298 nm; 229 and 231 nm). For the two other wavelengths, a greater number of MO is involved, and the transitions with preponderant contributions are no more identical, even if the calculated wavelengths are the same (201 nm). Finally, the introduction of the solvent effect does not have a significant impact on the theoretical spectrum of this free ligand.

Theoretical spectra of [Pb(3HF)]$^+$ have been calculated, as well in a vacuum as in methanol, with the two different pseudopotentials for lead (Lanl2dz and MWB78) from the corresponding optimized structures. In a vacuum, five bands are calculated in both spectra, leading to a very poor description of the experimental spectrum (Figure 2, part B). The greatest difference due to the pseudopotential used concerns the highest wavelength, which is calculated with MWB78 33 nm above the value obtained with Lanl2dz (469 nm), with this latter value being already far from $\lambda_{exptl} = 405$ nm. Thus, in a vacuum, the Lanl2dz pseudopotential gives relatively better results.

In methanol, discrepancies between pseudopotentials are almost canceled with respect to what is observed in a vacuum, with the major difference being of only 6 nm for the highest wavelength (Lanl2dz, 399 nm; MWB78, 405 nm). The peak calculated at 346 nm with MWB78 has a counterpart with Lanl2dz but with a too small oscillator strength to be plotted. One can note that all of the calculated bands correspond to the same transitions whatever the pseudopotential. The similarity between the theoretical spectra calculated in methanol with the two pseudopotentials is directly related to the relative energy of the molecular orbitals. In Table 4 are reported the energies of all the MOs involved in the plotted transitions. In a vacuum, all MOs have a higher energy with MWB78 than with Lanl2dz (+0.001 or 0.002 eV), except the LUMO which is lower by −0.004 eV. The HOMO−LUMO gap is then less important with MWB78, giving a too high value of the transition wavelength. This is no more the case in methanol. The only MO calculated with a lower energy with MWB78 than with Lanl2dz is L + 1 ($\Delta E = -0.001$ eV), which presents a low contribution in calculated transitions and therefore has a low impact on calculated wavelengths. If we consider the HOMO−LUMO gap, the values obtained with MWB78 and Lanl2dz are very comparable and differ by only 0.001 eV. It can be concluded that, in such calculations, the most important factor is the solvent effect, and not the pseudopotential used. The same calculations performed on the two other compounds lead to the same conclusions, and thus, in the following, only results obtained with the Lanl2dz pseudopotential will be presented.

Contrary to that observed for the free ligand, good agreement between experimental and theoretical absorption spectra of the complexed form is obtained only if the solvent effect is taken into account. Comparison of the experimental spectrum with that calculated with Lanl2dz in methanol is very satisfying. All of the observed bands are fairly reproduced by theoretical features, and some large and unstructured bands are assigned to several electronic transitions. Experimentally, upon complexation, the bands located at 302 and 344 nm in 3HF disappear and new bands appear at 266, 322, and 405 nm. All of these phenomena are nicely reproduced by the theoretical spectra. However, in fact, the calculations clearly show that only

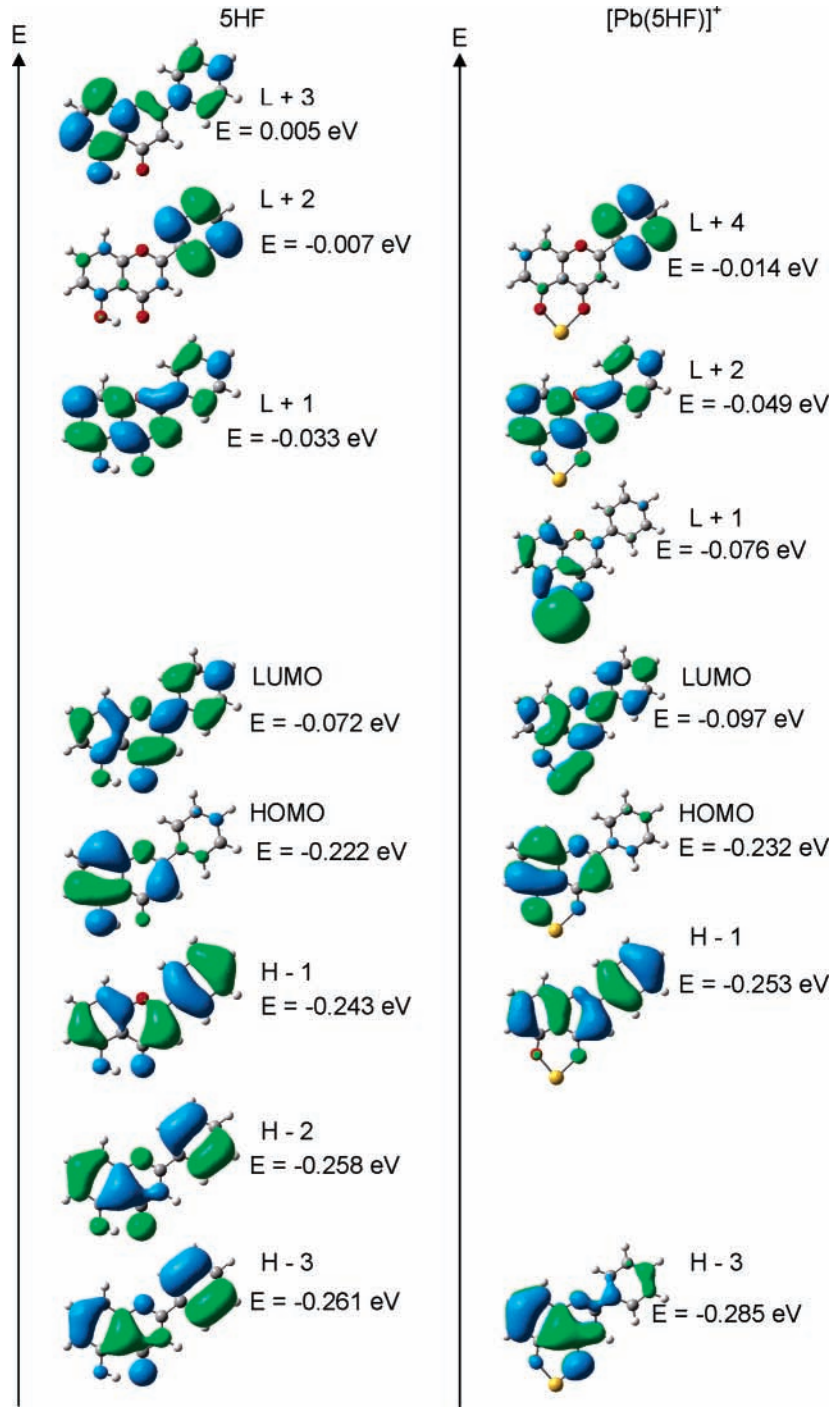

Figure 5. Molecular orbitals of 5HF and $[Pb(5HF)]^+$ calculated in methanol.

wavelength shifts are responsible for spectral modifications. This can be verified by looking at the shapes of the MOs involved in the considered transitions. The MOs of 3HF and $[Pb(3HF)]^+$ calculated in methanol are represented in Figure 3 (note that the MO shapes are identical in a vacuum and in methanol with both pseudopotentials for the complex). The MOs are reported in energetic order; however, the MOs having the same shape in free and complexed ligands are presented opposite each other. The L + 1 MO of $[Pb(3HF)]^+$, mainly localized on the Pb atom, has no counterpart in 3HF. From Figure 3 and Table 3, it is easy to see that the bands calculated at 351 and 298 nm in 3HF correspond to transitions between comparable MOs (preponderant contributions) in $[Pb(3HF)]^+$ at 399 and 332 nm, respectively. In the same way, the transition calculated at 282 nm in $[Pb(3HF)]^+$, assigned to the band observed at 266 nm, is the same as that calculated at 253 nm in 3HF (observed at 242 nm). The electronic absorption band in the long wavelengths is predominantly assigned to HOMO → LUMO (H → L) transition both in free and complexed forms. In the two cases, the transition consists of an electronic redistribution over the whole molecule and is not localized on a particular ring of flavonoids. The 6p orbital of lead(II) is involved in both the HOMO and LUMO of $[Pb(3HF)]^+$, but the transition does not reveal a metal−ligand charge transfer. Finally, the calculations fairly reproduce the bathochromic shift observed upon complexation, simply due to changes in MO energy. It is also interesting to notice that the L + 1 MO of $[Pb(3HF)]^+$, mainly localized on the lead ion, does not present a major contribution in electronic transitions.

TABLE 6: Experimental and Calculated[a] (in a Vacuum and in Methanol) Wavelengths (nm) for 3′,4′-diHF and Pb(3′,4′-diHF)[b]

3′,4′-diHF									Pb(3′,4′-diHF)								
	calcd									calcd							
exptl	vacuum					methanol			exptl	vacuum					methanol		
λ	λ	MO	%	f	λ	MO	%	f	λ	λ	MO	%	f	λ	MO	%	f
342	316	H → L	80	0.48	339	H → L	86	0.50	399	482	H → L	81	0.26	398	H → L	88	0.55
306					298	H − 1 → L	78	0.15	343	324	H → L + 1	82	0.31	355	H → L + 1	86	0.10
					284	H − 2 → L	82	0.11	301	277	H − 3 → L + 1	80	0.12	304	H − 1 → L + 1	79	0.14
					269	H → L + 1	84	0.18						288	H − 2 → L	66	0.14
244	246	H − 2 → L + 1	71	0.17	246	H − 1 → L + 1	59	0.15							H → L + 2	16	
						H → L + 2	13			266	H → L + 3	82	0.11	283	H → L + 2	66	0.18
213					215	H − 1 → L + 2	42	0.14							H − 2 → L	14	
						H − 4 → L + 1	30		237	246	H − 1 → L + 3	46	0.12	231	H → L + 5	31	0.20
201	204	H − 2 → L + 3	32	0.33	208	H − 1 → L + 3	65	0.31			H − 4 → L + 1	31			H − 2 → L + 2	29	
		H − 4 → L + 1	16			H − 2 → L + 2	14			217	H − 1 → L + 5	46	0.15	220	H − 1 → L + 4	85	0.20
		H − 3 → L + 3	15								H − 4 → L + 3	16					
									201	210	H − 3 → L + 5	20	0.16	206	H − 1 → L + 5	40	0.22
											H − 1 → L + 5	19			H → L + 7	36	
											H − 4 → L + 3	16					
											H − 8 → L	11					
										209	H − 1 → L + 6	60	0.17				
											H − 8 → L	12					

[a] Only transitions with an oscillator strength ≥0.1 and molecular orbitals with a contribution ≥10% are reported. [b] f: calculated oscillator strength.

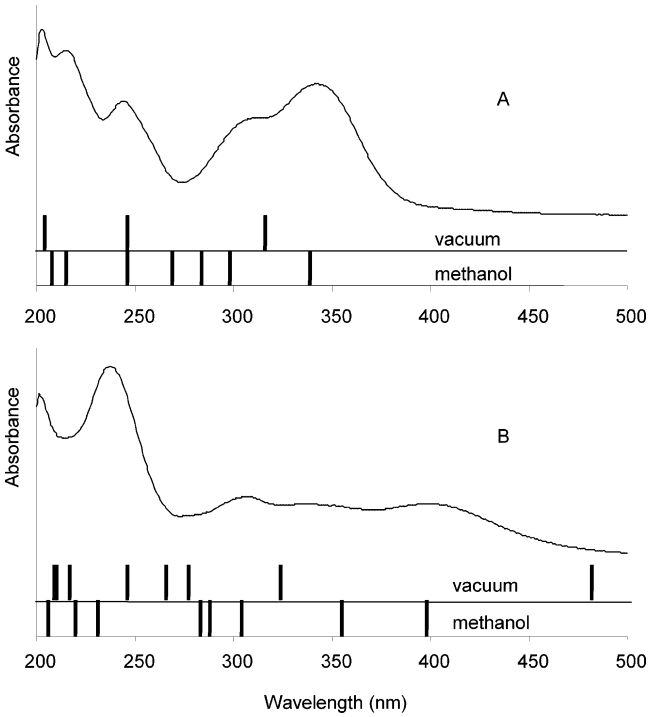

Figure 6. UV−visible spectrum recorded in methanol[23] and positions of the electronic transitions calculated in a vacuum and in methanol of (A) 3′,4′-diHF and (B) Pb(3′,4′-diHF).

5-Hydroxyflavone. The experimental and calculated spectra of 5HF and $[Pb(5HF)]^+$ are reported in Figure 4, parts A and B, respectively. For 5HF, the differences between calculated spectra in a vacuum and in methanol are more marked than those for 3HF. Indeed, there is not the same number of major transitions (oscillator strength ≥0.1) and only the H → L transition is common (Table 5). Better simulation of the UV−visible spectrum of 5HF is unambiguously obtained by calculations taking into account the solvent effect. In opposition to that observed for 3HF, the electronic density of the HOMO is localized on the chromone part of the molecule (A and C rings) (Figure 5), and the H → L transition, observed at 337 nm, is thus characterized by a charge transfer from the chromone moiety to the B ring.

For the complex, the theoretical spectrum calculated in a vacuum presents two major pitfalls: the absorption band located at 296 nm is not reproduced, and a transition is calculated at 379 nm, much higher than the extreme experimental wavelength of 335 nm. In methanol, the results are significantly better. All of the observed bands correspond to calculated transitions, and the greatest inaccuracy of the theoretical spectrum concerns λ_{exptl} = 296 nm, calculated at 280 nm. Once more, these results confirm the necessity to introduce the solvent effect to correctly simulate experimental features.

The experimental absorption spectra of 5HF and $[Pb(5HF)]^+$ are relatively similar. The main differences lie in the appearance of a new intense band localized at 241 nm in the spectrum of $[Pb(5HF)]^+$ and the disappearance of the shoulder located at 212 nm in the 5HF spectrum. These observations are well reproduced by the results obtained in methanol: the calculations lead to a new transition calculated at 244 nm in $[Pb(5HF)]^+$ and the loss of the band calculated at 210 nm in 5HF. Furthermore, the MOs predominantly involved in these two transitions (Table 5 and Figure 5) show that (i) the transition H − 1 → L + 2 calculated at 244 nm for $[Pb(5HF)]^+$ is not found in the theoretical spectrum of 5HF (the corresponding transition would be H − 1 → L + 1) and (ii) the transition H → L + 3 in 5HF (λ = 210 nm) is not found in the theoretical spectrum of $[Pb(5HF)]^+$ (where no counterpart to L + 3 is found). The three bands observed at 337, 298, and 270 nm in the electronic spectrum of 5HF are very close to those observed in that of $[Pb(5HF)]^+$ at 335, 296, and 268 nm, respectively. However, the theoretical results reported in Table 5 show that they cannot be assigned to the same transitions in both compounds. In fact, the H → L transition (located at 337 nm in 5HF) is calculated at 407 nm in $[Pb(5HF)]^+$ and not reported because of its low oscillator strength (0.06). However, a weak increase of the baseline, observed in the 400 nm range of the spectrum of the complex,[28] could be assigned to this transition (H → L). Thus, in the complexed form spectrum, the observed band of highest wavelength (335 nm) is assigned to the H → L + 1 transition, where L + 1 is a MO mainly localized on Pb. This absorption band corresponds to a charge transfer from the chromone part of the ligand to the metal. The band observed at 298 nm in 5HF (λ_{calcd} = 294 nm) shifts toward the band of highest wavelength (λ_{calcd} = 326 nm) in $[Pb(5HF)]^+$, λ_{calcd} = 275 nm

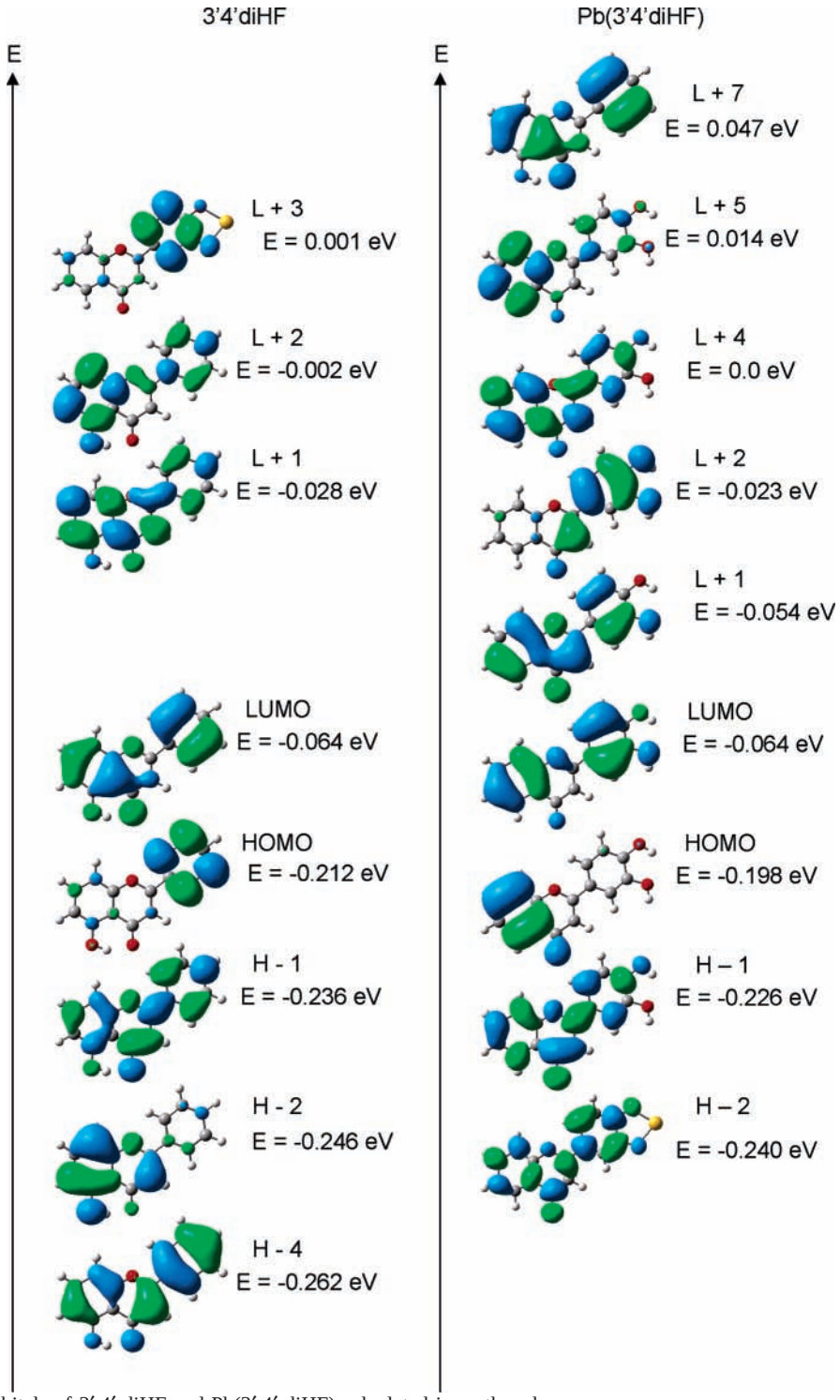

Figure 7. Molecular orbitals of 3′,4′-diHF and Pb(3′,4′-diHF) calculated in methanol.

in 5HF (λ_{exptl} = 270 nm) shifts to 280 nm (λ_{exptl} = 296 nm), and the transition observed and calculated at 268 nm in the complex is similar to that calculated at 262 nm in 5HF. Finally, even if the electronic absorption spectra of free and complexed ligands are very similar, assignment of the absorption bands is very different.

3′,4′-Dihydroxyflavone. The difference between theoretical spectra calculated in a vacuum and in methanol is drastic in 3′,4′-diHF (Figure 6A). Only three bands are calculated in a vacuum, whereas a minimum of five bands is observed in the UV−visible spectrum. In methanol, the results are much better, with a good agreement with all of the experimental features. The H → L transition assigned to the long wavelength band (Table 6) is mainly characterized by a charge transfer from the B ring to the A ring through the γ-pyrone moiety (Figure 7).

In Pb(3′,4′-diHF), introduction of the solvent effect is once more necessary to achieve a good representation of the experimental profile (Figure 6B). The theoretical spectrum calculated in a vacuum shows only one band between 300 and 400 nm, whereas three bands are recorded. Furthermore, the H → L transition is calculated at 482 nm (Table 6), very far from λ_{exptl} = 399 nm. In methanol, this latter transition is calculated at 398 nm, in good agreement with the experimental value. The two other bands in the high wavelength range are also fairly reproduced. In the low wavelength part, the three calculated

transitions can be easily assigned to the two observed profiles (Table 6). The HOMO, LUMO, and L + 1 MOs involve a nonnegligible participation of the 6p orbital of Pb(II). The HOMO of Pb(3′,4′-diHF) has exactly the same shape on the ligand that is observed for the HOMO of 3′,4′-diHF. In the same way, the LUMO and L + 1 orbitals of the complex are respectively obtained by in phase and in opposition phase associations of the HOMO of the ligand with the 6p atomic orbital of the metal.

Complexation of Pb(II) to the catechol group modifies notably the absorption spectra. Numerous shifts are observed. Only one common band is observed in both experimental spectra (201 nm) which corresponds to the same transition in the free and complexed ligands (Table 6, Figure 7). A bathochromic shift (57 nm) of the band assigned to the H → L transition is observed (calculated shift 59 nm) in the complex spectrum. The H → L transition in 3′,4′-diHF and the H → L + 1 transition in the complex present the same absorption maximum (342 and 343 nm, respectively). The bands observed at 306 and 213 nm in the free ligand shift to 301 and 237 nm in the complex, respectively. The transition corresponding to the 244 nm band in the 3′,4′-diHF spectrum has no equivalent in the complex.

4. Conclusion

In this contribution, we report for the first time the calculation of electronic spectra of lead(II) complexes of some hydroxyflavone molecules by the TD-DFT methodology. The results obtained by taking into account the solvent effect are in very good agreement with the experimental features and lead to a complete assignment of the spectral changes observed upon complexation of these compounds. This study also allows a better understanding of the behavior of the Pb(II) ion in relation to the three different chelating sites and confirms the deprotonation of hydroxyl groups occurring upon chelation.

If we compare the frontier orbitals of the three studied compounds, one can notice that the LUMO has almost the same shape in the three cases, whereas the HOMO shape presents a great dependence with respect to substitution. Indeed, a substitution on the A ring gives rise to an electronic localization on the A ring; in the same way, a substitution on the B ring leads to the localization of the electronic density on the B ring, and a substitution on the 3 position induces a complete delocalization on the entire molecule. For the frontier orbitals of the complexes, the electronic density on the ligand is the same as that observed on the corresponding free ligand. For the LUMOs, a contribution of lead always occurs and is preponderant only for Pb(3′,4′-diHF). In opposition, only the HOMO of $[Pb(5HF)]^+$ has no contribution of the 6p atomic orbital of the metal.

The nature and/or the probability of the H → L transition differ for each studied complex and could partially explain the different behaviors experimentally observed. For $[Pb(3HF)]^+$, the electronic delocalization on the whole molecule for these two MOs shows that there is no charge transfer in the transition. For both $[Pb(5HF)]^+$ and Pb(3′,4′-diHF), a complete charge redistribution is observed for the H → L transition, but this one is calculated for the 5HF complex with a very low oscillator strength and does not appear in the experimental spectrum, explaining that this compound is the only one to exhibit no bathochromic shift upon complexation.

Acknowledgment. "Institut du Développement et des Ressources en Informatique Scientique" (IDRIS, Orsay, France) is thankfully acknowledged for the CPU time allocation. The authors also thank the Lille University Computational Center (C.R.I.).

References and Notes

(1) Stevenson, F. J. *Humus Chemistry: Genesis, Composition, Reactions*; Wiley: New York, 1982.
(2) Aiken, G. R.; McKnight, D. M.; Warshaw, R. L.; MacCarthy, P. *Humic substances in soil, sediment and* water; Wiley: New York, 1985.
(3) Bartscahat, B. M.; Cabaniss, S. E.; Morel, F. M. M. *Environ. Sci. Technol.* **1992**, *26*, 284.
(4) Nederlof, M. M.; de Wit, J. C. M.; van Riemsdijk, W. H.; Koopal, L. K. *Environ. Sci. Technol.* **1993**, *27*, 846.
(5) Shin, H. S.; Rhee, S. W.; Lee, B. H.; Moon, C. H. *Org. Geochem.* **1996**, *24*, 523.
(6) Tipping, E. *Cation binding by Humic Substances*, 1st ed.; Cambridge University Press: Cambridge, U.K., 2002.
(7) Elkins, K. N.; Nelson, D. J. *Coord. Chem. Rev.* **2002**, *228*, 205.
(8) Forest, K.; Wan, P.; Preston, C. M. *Photochem. Photobiol. Sci.* **2004**, *3*, 463.
(9) Plaschke, M.; Rothe, J.; Denecke, M. A.; Fanghänel, T. *J. Electron. Spectrosc. Relat. Phenom.* **2004**, 135, 53.
(10) Giannakopoulos, E.; Christoforidis, K. C.; Tsipis, A.; Jerzykiewicz, M.; Deligiannakis, Y. *J. Phys. Chem. A* **2005**, *109*, 2223.
(11) Maria, P. C.; Gal, J. F.; Massi, L.; Burk, P.; Tanniku-Taul, J.; Tamp, S. *Rapid Commun. Mass Spectrom.* **2005**, *19*, 568.
(12) Coulson, C. B.; Davies, R. I.; Lewis, D. A. *J. Soil Sci.* **1960**, *11*, 20.
(13) Remko, M.; Polcin, J. *Collect. Czech. Chem. Commun.* **1980**, *45*, 201.
(14) Smith, D. S.; Kramer, J. R. *Environ. Int.* **1999**, *25*, 295.
(15) Smith, D. S.; Kramer, J. R. *Anal. Chim. Acta* **2000**, *416*, 211.
(16) Haslam, E. *Plant Polyphenols. Vegetable Tannins Revisited*; Cambridge University Press: Cambridge, U.K., 1989.
(17) Larson, R. A. *Phytochemistry* **1988**, *27*, 969.
(18) Pszonicki, L.; Tkacs, W. *Anal. Chim. Acta* **1976**, *87*, 177.
(19) Wang, Z. P.; Shi, L. L.; Chen, G. S.; Cheng, K. L. *Talanta* **2000**, *51*, 315.
(20) Takamura, K.; Sakamoto, M. *Chem. Pharm. Bull.* **1978**, *26*, 2291.
(21) Boudet, A. C.; Cornard, J. P.; Merlin, J. C. *Spectrochim. Acta* **2000**, *56*, 829.
(22) Cornard, J. C.; Boudet, A. C.; Merlin, J. C. *Spectrochim. Acta* **2001**, *57*, 591.
(23) Cornard, J. P.; Merlin, J. C. *J. Mol. Struct.* **2001**, *569*, 129.
(24) Cornard, J. P.; Merlin, J. C. *J. Inorg. Biochem.* **2002**, *92*, 19.
(25) Cornard, J. P.; Merlin, J. C. *Polyhedron* **2002**, *21*, 2810.
(26) Cornard, J. P.; Merlin, J. C. *J. Mol. Struct.* **2003**, *651*, 381.
(27) Boilet, L.; Cornard, J. P.; Lapouge, C. *J. Phys. Chem. A* **2005**, *109*, 1952.
(28) Dangleterre, L.; Cornard, J. P. *Polyhedron*, in press.
(29) Gampp, H.; Maeder, M.; Meyer, C. J.; Zuberbühler, A. *Talanta* **1986**, *33*, 943.
(30) Frisch, M. J.; Trucks, G. W.; Schlegel, H. B.; Scuseria, G. E.; Robb, M. A.; Cheeseman, J. R.; Zakrzewski, V. G.; Montgomery, J. A., Jr.; Stratmann, R. E.; Burant, J. C.; Dapprich, S.; Millam, J. M.; Daniels, A. D.; Kudin, K. N.; Strain, M. C.; Farkas, O.; Tomasi, J.; Barone, V.; Cossi, M.; Cammi, R.; Mennucci, B.; Pomelli, C.; Adamo, C.; Clifford, S.; Ochterski, J.; Petersson, G. A.; Ayala, P. Y.; Cui, Q.; Morokuma, K.; Malick, D. K.; Rabuck, A. D.; Raghavachari, K.; Foresman, J. B.; Cioslowski, J.; Ortiz, J. V.; Stefanov, B. B.; Liu, G.; Liashenko, A.; Piskorz, P.; Komaromi, I.; Gomperts, R.; Martin, R. L.; Fox, D. J.; Keith, T.; Al-Laham, M. A.; Peng, C. Y.; Nanayakkara, A.; Gonzalez, C.; Challacombe, M.; Gill, P. M. W.; Johnson, B. G.; Chen, W.; Wong, M. W.; Andres, J. L.; Head-Gordon, M.; Replogle, E. S.; Pople, J. A. *Gaussian 98*, revision B.04; Gaussian, Inc.: Pittsburgh, PA, 1998.
(31) Becke, A. D. *J. Chem. Phys.* **1993**, *98*, 5648.
(32) Lee, C.; Yang, W.; Parr, R. G. *Phys. Rev. B* **1988**, *37*, 785.
(33) Bauernschmitt, R.; Ahlrichs, R. *Chem. Phys.* **1996**, *256*, 454.
(34) Cossi, M.; Scalmani, G.; Rega, N.; Barone, V. *J. Chem. Phys.* **2002**, *117*, 43.
(35) Meyer, M. *Int. J. Quantum Chem.* **2000**, *76*, 724.
(36) Petroski, J. M.; De Sa Valente, C.; Kelson, E. P.; Collins, S. *J. Phys. Chem. A* **2002**, *106*, 11714.
(37) Premvardhan, L. L.; Peteanu, L. A. *J. Phys. Chem. A* **1999**, *103*, 7506.
(38) Alluis, B.; Dangles, O. *Helv. Chim. Acta* **1999**, *82*, 2201.
(39) Katyal, M.; Prakash, S. *Talanta* **1977**, *24*, 367.
(40) Browne, B. A.; McColl, J. G.; Driscoll, C. T. *J. Environ. Qual.* **1990**, *19*, 65.
(41) Urbach, F. L.; Timnick, A. *Anal. Chem.* **1968**, *40*, 1269.
(42) Zhou, J.; Wang, L.; Wang, J.; Tang N. *J. Inorg. Biochem.* **2001**, *83*, 41.
(43) Salpin, J. Y.; Tortajada, J.; Alcami, M.; Mo, O.; Yanez, M. *Chem. Phys. Lett.* **2004**, *383*, 561.